



Investigation on mining-induced fractured zone height developed in different layers above Jurassic coal seam in western China

Shiliang Liu¹ · Wenping Li¹ · Qiqing Wang¹ · Yabing Pei²

Received: 30 June 2017 / Accepted: 2 January 2018 / Published online: 11 January 2018
© Saudi Society for Geosciences 2018

Abstract

The mining-induced fractured zone height (MIFZH) is of significant importance for water hazard prevention and regional eco-environmental conservation in the Jurassic coal field of western China. The paper discussed MIFZH developed in bedrock and Neogene laterite from two aspects of field measurement and theoretical analysis respectively. In theoretical analysis of MIFZH developed in bedrock, based on plate and shell theory, each stratum in bedrock above the coalface stress-decreasing zone was simplified as four clamped rectangular plates, and the value of the ultimate deflection of the thin plate and the height of the free space in the lower part of the stratum were compared to judge MIFZH. When MIFZH was developed in Neogene laterite, MIFZH was calculated by Pu's theory and rock mass limit equilibrium theory in theoretical analysis; in on-site measurement, micro resistivity scanning imaging logging technology (MRSILT), overcoming the shortage of fluid leakage technology, was adopted to detect MIFZH, where its measured result proved the feasibility of theoretical analysis. The research results have important significance to water conservation mining and safety mining of the Jurassic coal seam in western China.

Keywords MIFZH · Bedrock · Neogene laterite · Theoretical analysis · On-site measurement

List of symbols

γ The bulk density of overlying strata
 H The buried depth of overlying strata
 $q_1(x)$ The linear triangular load caused by mining pressure in stress reduction zone

$q(x)$ The lateral total load on the rectangular thin plate
 a The strike length of overlying strata
 b The width of overlying strata
 D The bending stiffness of a thin plate
 h_i The thickness of overlying each stratum
 ν Poisson's ratio of strata
 E Elastic module of strata
 a_m The thin plate limit span of strike length
 b_m The thin plate limit span of inclined length
 k The shape coefficient of a thin plate
 S_i The free space height of the i^{th} layer stratum
 M The mining thickness of coal seam
 K_j The broken expansion coefficient of the j^{th} layer stratum
 ω_j Ultimate deflection of a thin plate
 σ_t Tensile strength
 f_k Firmness coefficient
 d The half of strike span of equilibrium arch in laterite
 F Horizontal reaction force
 V Vertical reaction force
 H_g The distance from the top boundary of equilibrium arch to surface
 h_b Bedrock thickness
 h_{li} Mining-induced fractured zone height

Electronic supplementary material The online version of this article (<https://doi.org/10.1007/s12517-018-3383-z>) contains supplementary material, which is available to authorized users.

✉ Wenping Li
wpligroup@sohu.com

Shiliang Liu
liushiliang0537@163.com

Qiqing Wang
qiqw89@qq.com

Yabing Pei
454937119@qq.com

¹ School of Resources and Geosciences, China University of Mining and Technology, Xuzhou 221116, China

² Nuclear Industry Huzhou Engineering Survey Institute, Huzhou 313000, China

Introduction

For the past few years, the focus of coal resource exploitation in China has been transferred to the arid and semi-arid regions with fragile ecological environment in western China. The large-scale development of coal industry, seriously affecting the sustainable development of regional economy and social stability, has been aggravating the damage of ecological environment, including water shortages, vegetation death, and intensified desertification (Zhang et al. 2009; Li et al. 2000a, b; Zhang and Dang 2014; Liu et al. 2017; Qiao et al. 2017). Therefore, the accurate determination of mining-induced fractured zone height (MIFZH), realizing the water conservation mining, has important theoretical and practical significance to the safe mining and ecological environment protection in western China.

Scholars, putting forward the scope and rules of overburden failure, calculating the empirical formulas of MIFZH, and proposing the safety measures of water conservation mining, have done a lot of research on overburden failure and formation of water conducting channel. Field test was used to determine MIFZH in practice engineering by fluid leakage technology (Sun et al. 2009) and by radon detection technology characterized by poor operability (Zhang et al. 2014). Additionally, scholars established the empirical formula and proposed the evaluation methods according to the measured results (Chai and Li 2014; Hu et al. 2012; Ning et al. 2015; Wei et al. 2016a, b; Wu et al. 2016a, b). Further, MIFZH was determined by physical similarity simulation test (Miao et al. 2011; Xu et al. 2009) and numerical simulation software, such as RFPA (rock failure process analysis system) (Chen et al. 2006; Fan et al. 2011), FLAC^{3D} (Liu et al. 2015), PFC (Wang et al. 2016), and UDEC (Zhang et al. 2016). In terms of theoretical research, Wang et al. (2012) predicted the height of water-flowing fractured zone for shallow seam covered with bedrock and thick windblown sands based on key strata theory. Gao (1996), Gao et al. (2012) proposed the concept of interlayer stratum and “four-zone” model of rock mass movement. Zhao et al. (2015) and Shi et al. (2012) determined the relationship between MIFZH and mining parameters, which were successfully applied in mining practice. Majdia et al. (2012) proposed five mathematical models to calculate water flowing fractured height in longwall mining. Palchik (2003) studied the formation process and extents of zones of interconnected and separate fractures in overburden caused by the active longwall coal mines in the Ukraine area.

Although these above results are of great significance for water conservation mining, there are still the following problems. (1) The top boundary of MIFZH was developed in bedrock in above literatures, not developed in soil layer. (2) In terms of field test, when MIFZH was developed in bedrock, it is reasonable to adopt fluid leakage technology to judge MIFZH. But when MIFZH was developed in soil layer, due to the closing effect and self-made slurry in soil layer (Li et al.

2011), fluid leakage technology shows varying degrees of technical bottlenecks, causing the difficulty in determining MIFZH.

For these reasons, the paper discussed MIFZH developed in bedrock and Neogene laterite from two aspects of field measurement and theoretical analysis respectively. In theoretical analysis of MIFZH developed in bedrock, the formula for calculating MIFZH was obtained based on plate and shell theory. When MIFZH was developed in Neogene laterite, MIFZH was calculated by Pu’s theory and rock mass limit equilibrium theory in theoretical analysis; in on-site measurement, a new measurement technology, overcoming the shortage of fluid leakage technology, was introduced to detect MIFZH.

Survey region

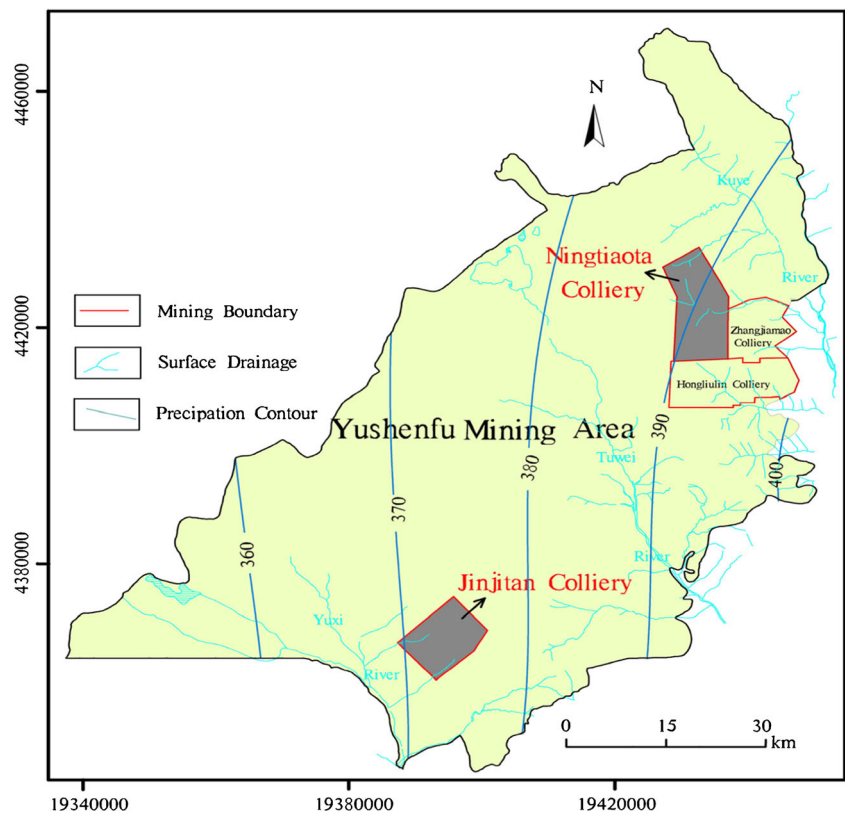
With the deepening development of western regions and China’s energy strategy westward, Yushenfu mining area as the base of energy function is also highlighted, which is rich in coal resources. Yushenfu mining area is located in the border zone between Maowusu Desert in western China and the Loess Plateau in Northern Shaanxi, which belongs to the arid and semi-arid continental monsoon climate, with less than 400 mm of the average annual rainfall (Fig. 1) and 1700~2500 mm of the average annual evaporation (Zhang et al. 2014). What is more, the area of rivers and valleys is affected by seasonal changes, in which available rivers and valleys are less. Therefore, water shortages, intensified desertification, and fragile geological and ecological environment of this region becomes the key area of soil and water conservation and desertification control.

From top to bottom, the stratigraphic succession consists of Quaternary (Aeolian sand, loess), Neogene (laterite), and Jurassic (An’ding, Zhiluo, and Yan’an formation). The main minable seam is the No. 2, which belongs to the Jurassic Yan’an formation. The overburden strata are shown in Fig. 2. Because of shallow buried coal seam, MIFZH was developed in different layer (Fig. 2). Based on the measured data, the paper discussed the MIFZH in bedrock and Neogene laterite, which developed in Ningtiaota colliery and Jinjitan colliery.

MIFZH developed in bedrock

Taking 12-2^{up}0101 coalface of Jinjitan colliery in Yushenfu mining area as engineering background, the authors analyzed MIFZH in bedrock from two aspects of field measurement and theoretical analysis respectively. The buried depth of coal seam in 12-2^{up}0101 coalface is 266.2 m, and the mining thickness is 5.5 m. In addition, the bedrock thickness is 215.26 m.

Fig. 1 Location of survey region



Theoretical analysis

Calculating ultimate deflection of strata

Before coal seam mining, the surrounding rock is in the balance state of natural stress. After coal seam mining,

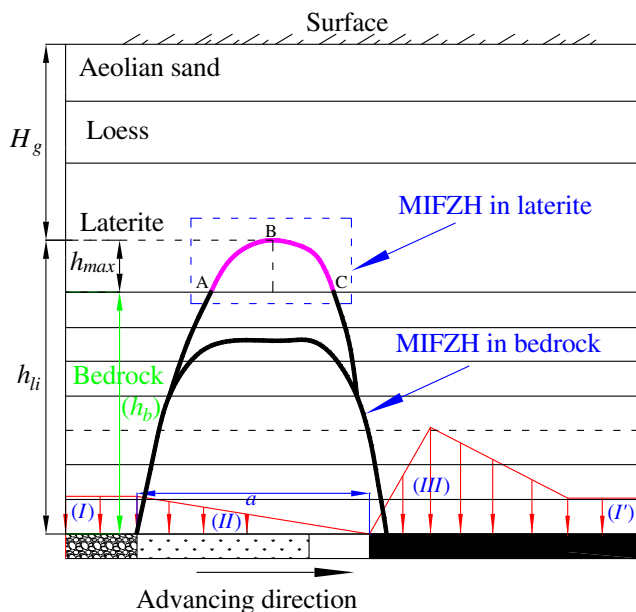


Fig. 2 Diagrammatic sketch of abutment pressure distribution and MIFZH in different layers

the abutment pressure of coalface can be divided into the stress reduction zone (II), the stress increasing zone (III), and the stress invariant zone (I and I') (Qian et al. 2010), as shown in Fig. 2. This paper took each layer of bedrock above the stress reduction zone as the research object. According to the mining practice of large-scale longwall coalface in western China, the overlying each stratum thickness is much less than the strike length of the stress reduction zone of coalface, that is, the ratio of the thickness of overlying each stratum and the strike length of the stress reduction zone (a) is less than $1/5$. Therefore, overlying each stratum in bedrock can be regarded as the rectangular thin plate with completed clamped and then the thin plate theory can be applied (Xu 1982). Figure 3 showed the thin plate mechanical model of each stratum of overlying bedrock.

In Fig. 3, the X and Y coordinate axes were arranged on the upper surface of each stratum of overlying bedrock along the strike and inclined direction of coalface, respectively, and the point of intersection is O . The lateral load on a stratum is composed of two parts. One part is the weight of the overlying strata, γH , where γ is the bulk density of overlying a stratum, KN/m^3 ; H is the buried depth of overlying a stratum, m . The other part is the stress reduction zone caused by mining pressure, which can be simplified as a linear triangular load, $q_1(x) = \gamma H(1 - x/a)$, where x is the distance to the point O along the X coordinate axes. The

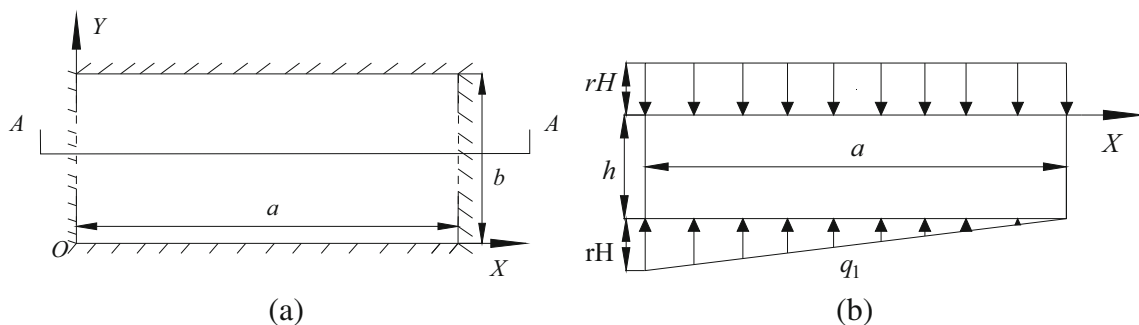


Fig. 3 Mechanical model of a stratum in bedrock. a Top view. b A-A section

lateral total load on the rectangular thin plate with completed clamped is $q(x) = \gamma Hx/a$.

The boundary conditions of the thin plate mechanical model of overlying each stratum in Fig. 3 are as follows:

$$\begin{cases} (\omega)_{x=0} = 0, \left(\frac{\partial^2 \omega}{\partial x^2}\right)_{x=0} = 0 \\ (\omega)_{x=a} = 0, \left(\frac{\partial^2 \omega}{\partial x^2}\right)_{x=a} = 0 \\ (\omega)_{y=0} = 0, \left(\frac{\partial^2 \omega}{\partial y^2}\right)_{y=0} = 0 \\ (\omega)_{y=b} = 0, \left(\frac{\partial^2 \omega}{\partial y^2}\right)_{y=b} = 0 \end{cases} \quad (1)$$

It was assumed that the deflection function of overlying each stratum is Eq. (2) based on double trigonometric series method and a linear load on the thin plate (Huang 1987):

$$\omega = \sum_{m=1}^{\infty} \sum_{n=1}^{\infty} A_{mn} x \sin^2\left(\frac{m\pi x}{a}\right) \sin^2\left(\frac{n\pi y}{b}\right) \quad (2)$$

where m and n are positive integers. It is proved that the deflection function satisfies the boundary conditions (Supplemental material). The coefficient of the deflection function A_{mn} can be calculated based on the principle of minimum potential energy (Xu 1982), as shown in the Eq. (3):

$$A_{mn} = \frac{\gamma Ha \left(\frac{2}{3} - \frac{1}{m^2 \pi^2}\right)}{2D \left[\left(\frac{m\pi}{b}\right)^4 a^2 \left(1 - \frac{15}{8m^2 \pi^2}\right) + \left(\frac{m\pi}{a}\right)^2 \left(m^2 \pi^2 + \frac{15}{8}\right) + \left(\frac{n\pi}{b}\right)^2 \left(\frac{2}{3} m^2 \pi^2 - \frac{1}{4}\right) \right]} \quad (3)$$

where a is the strike length of overlying each stratum, that is, strike length of stress reduction zone of coalface, m ; b is the width of overlying each stratum, m ; D is bending stiffness of the thin plate, $D = \frac{Eh_i^3}{12(1-\nu^2)}$; h_i is the thickness of a stratum, m ; ν is Poisson's ratio of a stratum; E is elastic module of a stratum, MPa.

Hence, the deflection function of overlying each stratum is shown in Eq. (4):

$$\omega = \sum_{m=1}^{\infty} \sum_{n=1}^{\infty} \frac{\gamma Ha \left(\frac{2}{3} - \frac{1}{m^2 \pi^2}\right) x \sin^2\left(\frac{m\pi x}{a}\right) \sin^2\left(\frac{n\pi y}{b}\right)}{2D \left[\left(\frac{m\pi}{b}\right)^4 a^2 \left(1 - \frac{15}{8m^2 \pi^2}\right) + \left(\frac{m\pi}{a}\right)^2 \left(m^2 \pi^2 + \frac{15}{8}\right) + \left(\frac{n\pi}{b}\right)^2 \left(\frac{2}{3} m^2 \pi^2 - \frac{1}{4}\right) \right]} \quad (4)$$

Due to the rapid convergence of the series in Eq. (4), the paper selected $m = n = 1$ for simplifying the calculation, and it is proved that the results can meet the requirements of the accuracy of the project. Therefore, the deflection function is shown in Eq. (5):

$$\omega = \frac{\gamma Ha \left(\frac{2}{3} - \frac{1}{\pi^2}\right)}{2D \left[\left(\frac{\pi}{b}\right)^4 a^2 \left(1 - \frac{15}{8\pi^2}\right) + \left(\frac{\pi}{a}\right)^2 \left(\pi^2 + \frac{15}{8}\right) + \left(\frac{\pi}{b}\right)^2 \left(\frac{2}{3} \pi^2 - \frac{1}{4}\right) \right]} x \sin^2\left(\frac{\pi x}{a}\right) \sin^2\left(\frac{\pi y}{b}\right) \quad (5)$$

The maximum deflection function of plate-shaped strata does not mean that the strata are in a failure state. So, it is necessary to calculate the ultimate deflection of plate-shaped strata. It is assumed that the thin rock plate limit span of strike and inclined length is a_m, b_m , respectively, which depends on their physical and mechanical properties of rocks, thickness, load, and other factors. The failure condition of thin plate is when tensile strength σ_t is greater than ultimate tensile strength $[\sigma_t]$, and the thin plate is broken. At this time, a_m, b_m of the thin plate size is limit size. The computational formula derived based on the tensile strength was shown in Eq. (6) (Huang 1987):

$$a_m = ab_m/b \quad (6)$$

where $b_m = \sqrt{\sigma_t h^2 / (6kq)}$, k is shape coefficient of thin plate, $k = 0.00302(a/b)^3 - 0.03567(a/b)^2 + 0.13953(a/b) - 0.05859$.

Therefore, the ultimate deflection function of overlying each stratum was shown in Eq. (7):

$$\omega_j = \frac{\gamma Ha_m \left(\frac{2}{3} - \frac{1}{\pi^2}\right)}{2D \left[\left(\frac{\pi}{b_m}\right)^4 a_m^2 \left(1 - \frac{15}{8\pi^2}\right) + \left(\frac{\pi}{a_m}\right)^2 \left(\pi^2 + \frac{15}{8}\right) + \left(\frac{\pi}{b_m}\right)^2 \left(\frac{2}{3} \pi^2 - \frac{1}{4}\right) \right]} x \sin^2\left(\frac{\pi x}{a_m}\right) \sin^2\left(\frac{\pi y}{b_m}\right) \quad (7)$$

Judging MIFZH

The free space formed after coal seam mining will be filled with the broken expansion characteristics of the overlying strata. The free space height of a stratum can be obtained from Eq. (8) if the caving zone and the fracture zone have broken expansion characteristic and while the bending zone does not:

$$S_i = M - \sum_{j=1}^{i-1} h_j (k_j - 1). \quad (8)$$

where S_i is the free space height of the i th layer stratum, m ; M is the mining thickness of coal seam, m ; h_j is the thickness of the j th layer stratum, m ; K_j is the broken expansion coefficient of the j th layer stratum. Based on mining practice, the broken expansion coefficient of mudstone and sandstone is 1.035 and 1.03, respectively.

MIFZH depends on the ultimate deflection value of a stratum ω_{jmax} and its lower free space height S_i . If $\omega_{jmax} < S_i$, a stratum will be broken, making MIFZH increase. On the contrary, the height of MIFZH will be stable.

Analysis of theoretical results

Based on drilling core data, Table 1 shows the characteristics and physical and mechanical parameters of overlying strata in 12-2^{up}0101 coalface. Taking the 2nd layer (drilling depth from 244.9 to 260 m) and 13th layer (drilling depth from 138.5 to 139.64 m) of overlying strata above coal seam as example, the authors made a theoretical calculation according to the above-established method of MIFZH.

Firstly, the free space height of the 2nd layer stratum was calculated.

$$S_2 = 5.5 - 6.2 \times (1.03 - 1) = 5.283 \text{ m}$$

Similarly, the free space height of the 13th layer stratum was calculated.

$$S_{13} = 5.5 - \sum 120.36 \times (1.035 - 1) - \sum (6.2 + 9.02) \times (1.03 - 1) = 1.146 \text{ m}$$

Secondly, the limit size of the 2nd layer and the 13th layer was $a_{m2} = b_{m2} = 35.85 \text{ m}$ and $a_{m13} = b_{m13} = 9.98 \text{ m}$, respectively.

Thirdly, the ultimate deflection ω_{jmax} of the 2nd layer and the 13th layer was calculated. 3D surface maps of ultimate deflection function in the 2nd layer and the 13th layer was obtained based on Eq. (7) and the mathematical engineering software MathCAD (Juan 1996), as shown in Fig. 4, where ultimate deflection of the 2nd layer and the 13th layer was 3.37 and 1.67 m, respectively.

At last, the values of ultimate deflection and the free space height in the same layer were compared in order to judge

MIFZH. In the second layer stratum, $\omega_{jmax2} = 3.37 \text{ m} < S_2 = 5.283 \text{ m}$, that is, the second layer is in failure state. In the 13th layer stratum, $\omega_{jmax13} = 1.67 \text{ m} < S_{13} = 1.146 \text{ m}$, that is, the 13th layer is not destroyed.

In the same way, the failure state of each rock stratum is shown in Table 1. After calculation, MIFZH was 126.56 m.

On-site measurement

Fluid leakage technology by ground drilling was adopted to detect MIFZH of 12-2^{up}0101 coalface in Jinjitan colliery. Drilling JT4 is located in the central position of the strike and inclined direction of coalface, which was drilled after the coal seam had been mined for 3 months, and the overlying strata was stable; therefore, MIFZH had reached its maximum value. MIFZH was determined by observing the fluid leakage and water level in drilling in the process of drilling. The analysis process and results were as follows.

1. Fluid leakage and water level in drilling

Table 1 showed the curve between fluid leakage, water level, and drilling depth. With the range value from 0.129 to 0.363 l/s and average value 0.193 l/s, fluid leakage was measured after the drill entered into bedrock, which illustrated that there is no fracture induced by mining in this section. When drilling depth reached 139.8 m, fluid leakage suddenly increased to 0.626 l/s, while the borehole water level was also greatly reduced, which existed fractured induced by mining. With the range value from 0.386 to 0.840 l/s and average value 0.592 l/s, liquid leakage showed the trend of fluctuation in 160.20~167.16 m borehole section, while the borehole water level was slowly decreasing. When drilling depth reached 168.8 m, flush liquid totally leaked and the borehole water level was still slowly decreasing until no water level in drilling depth 202.31 m.

2. Determining MIFZH

The depth of 139.8 m was considered as top boundary of MIFZH based on the above analysis. What is more, the buried depth of coal seam was 266.2 m, and therefore, MIFZH was 126.4 m.

Developed in bedrock, MIFZH was 126.56 and 126.4 m in theoretical analysis and field test, respectively, which the two results were basically consistent and verified the feasibility of theoretical analysis.

MIFZH developed in Neogene laterite

Taking N1206 coalface of Ningtiaota colliery in Yushenfu mining area as engineering background, authors analyzed

Table 1 Characteristics, physical and mechanical parameters, and failure state of the overlying strata

Column	Layer thickness (m)	Gross thickness (m)	Name	Tensile strength (MPa)	Bulk density (kN/m ³)	Elastic modulus (MPa)	Poisson ratio	Theoretical Calculation			Failure state	On-site Measurement	
								$a_m(b_m)$ (m)	Q_{jmax} (m)	S_s (m)		Curve between fluid leakage and depth	Curve between water level and depth
											0 1.0 2.0 3.0 4.0 L/s	0 50 100 150 200 m	
	3.0	3.0	AS	—	—	—	—	—	—	—	—		
	17.54	20.54	Loess	—	—	—	—	—	—	—	—		
	8.9	134.2	MGS	11	25.4	7500	0.28	20.06	1.89	0.695	No Failure		
	1.3	135.5	MS	15	23.8	8700	0.35	6.25	1.51	1.007	No Failure		
	3.0	138.5	SS	12	27.2	6100	0.26	9.58	1.26	1.112	No Failure		
	1.14	139.64	MS	10.7	23	9100	0.33	9.98	1.67	1.146	No Failure		
	9.02	148.66	FS	9.3	25	8800	0.33	25.21	1.39	1.462	Failure		
	14.34	163	MGS	9.5	23.3	8900	0.36	37.85	1.68	1.964	Failure		
	5.30	168.3	SS	10.5	26.1	7400	0.29	14.47	1.11	2.149	Failure		
	14.27	182.57	FS	11	25.5	9200	0.31	36.26	1.55	2.648	Failure		
	7.73	190.3	MGS	11	23.2	9000	0.30	20.39	1.15	2.919	Failure		
	10.91	201.21	FS	9.1	25.6	8600	0.29	23.91	1.83	3.301	Failure		
	7.09	208.3	SS	11	26.4	7500	0.26	18.38	1.52	3.549	Failure		
	6.55	214.85	FS	10	26.1	6800	0.25	16.43	1.39	3.778	Failure		
	11.05	225.9	SS	9.2	24.9	7400	0.30	26.57	1.74	4.165	Failure		
	19	244.9	FS	9.9	24.6	8500	0.29	42.54	2.04	4.83	Failure		
	15.1	260	MGS	9	28.2	6600	0.25	35.85	3.37	5.283	Failure		
	6.2	266.2	MS	9.5	28	6900	0.30	13.17	0.87	5.5	Failure		
	5.5	271.7	2 ² CS	—	14.2	420	0.31	—	—	—	—		
	12.3	284	FS	9.2	25.6	7800	0.29	—	—	—	—		

AS Aeolian Sand, MGS medium-grained sandstone, MS mudstone, SS silt sandstone, FS fine sandstone, CS coal seam

MIFZH in Neogene laterite from two aspects of field measurement and theoretical analysis, respectively. The buried depth of coal seam in N1206 coalface is 219.53 m, and the mining thickness is 4.8 m.

Theoretical analysis

Calculating critical height in Neogene laterite

When MIFZH penetrated bedrock into Neogene laterite, laterite was broken continuously from the bottom to the top. If the thickness of the soil layer is large enough, when the soil layer is destroyed to a critical height, a natural equilibrium arch is formed, and the soil layer will not continue to be destroyed (Fig. 2). Hence, Pu’s theory (Tan and Xian 1994) was adopted to calculate critical height in Neogene laterite. The theoretical calculation steps are as follows.

1. When MIFZH was developed to the interface between bedrock and laterite, width of bedrock surface damage was calculated based on overlying strata breaking angle (Yan 2013), which was regarded as strike span of equilibrium arch in laterite.

2. Calculating critical height of equilibrium arch in Neogene laterite

In Fig. 2, equilibrium arch in laterite was extracted, as shown in Fig. 5, where the AB section of the equilibrium arch was made a force analysis. Vertical uniform load G acts on the arch. The force of the BC segment on the AB segment is horizontal tangential support force T at B point. Horizontal reaction force F and vertical reaction force V act on the A point. The AB section of the arch is in balance state under the joint action of the above forces, as shown in Eq. (9):

$$\begin{cases} \sum F_y = 0 \\ \sum F_x = 0 \\ \sum M_A = 0 \end{cases} \tag{9}$$

Because the arch is in the limit equilibrium state, horizontal reaction force F and the friction produced by vertical reaction force V are in balance state, that is,

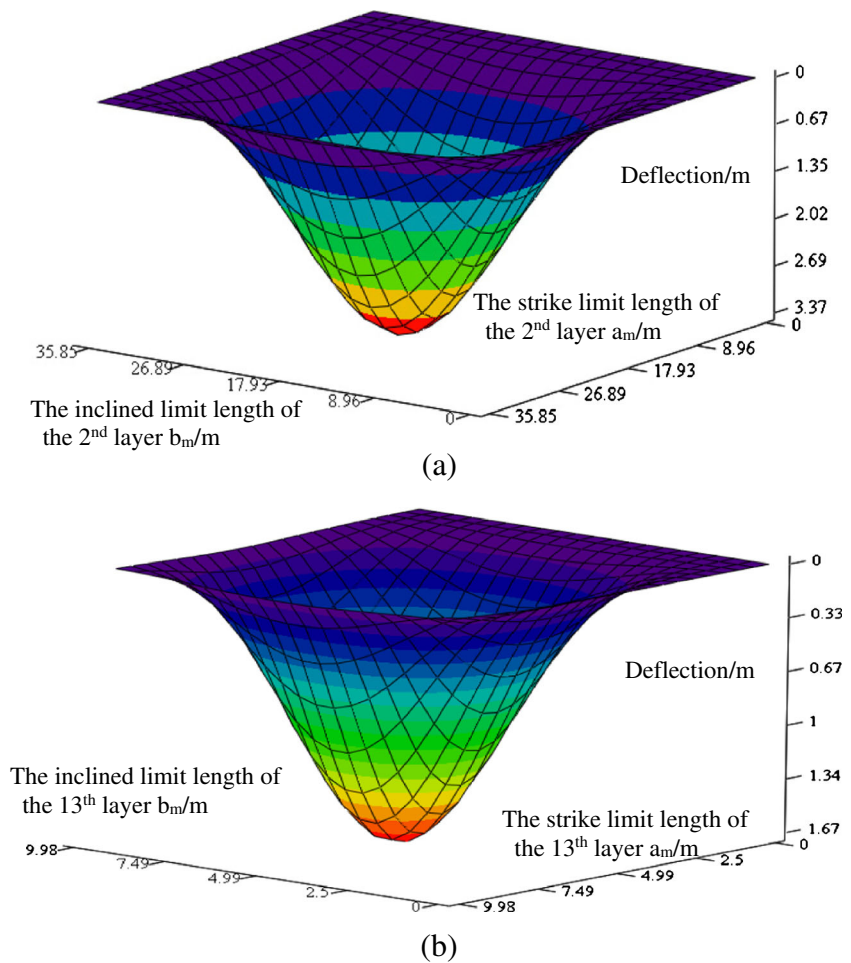
$$F = V f_k \tag{10}$$

where f_k is firmness coefficient.

To ensure adequate stability of the arch in the horizontal direction, $F > T$ is required. That is, $T < V f_k, f_k$ takes 2. That is,

$$2T = V f_k \tag{11}$$

Fig. 4 3D surface map of ultimate deflection function. **a** The 2nd layer. **b** The 13th layer



Based on Eqs. (9), (10), and (11), the critical height is shown in Eq. (12).

$$h_{max} = d/f_k \tag{12}$$

where d is half of strike span of equilibrium arch in laterite.

3. If there is a stable equilibrium arch in laterite, Eq. (13) must be satisfied:

$$H_g \geq 2h_{max} \tag{13}$$

where H_g is the distance from the top boundary of equilibrium arch to surface.

4. MIFZH is calculated as follows:

$$h_{li} = h_{max} + h_b \tag{14}$$

where h_b is bedrock thickness.

Analysis of theoretical results

MIFZH of N1206 coalface in Ningtiaota colliery was calculated based on the above theoretical calculation method. The analysis process was as follows.

1. Bedrock breaking angle is chosen 55° based on mining practice and lithology strength. Bedrock thickness is 120.67 m. Therefore, strike span of equilibrium arch in laterite is 60.66 m.

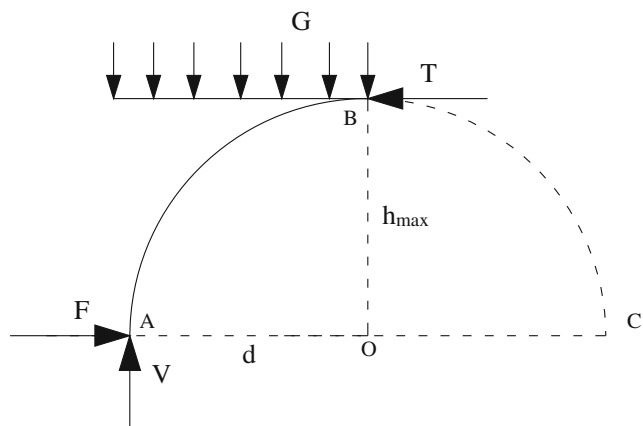


Fig. 5 Stress diagram of equilibrium arch

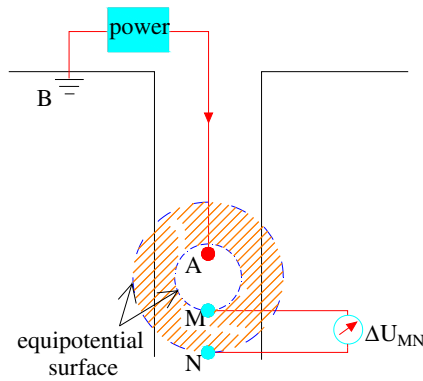


Fig. 6 Schematic map of MRSILT

2. According to literature (Yao and Zhu 2012), firmness coefficient of laterite $f_k = 1$. So, $h_{max} = 30.33$ m.

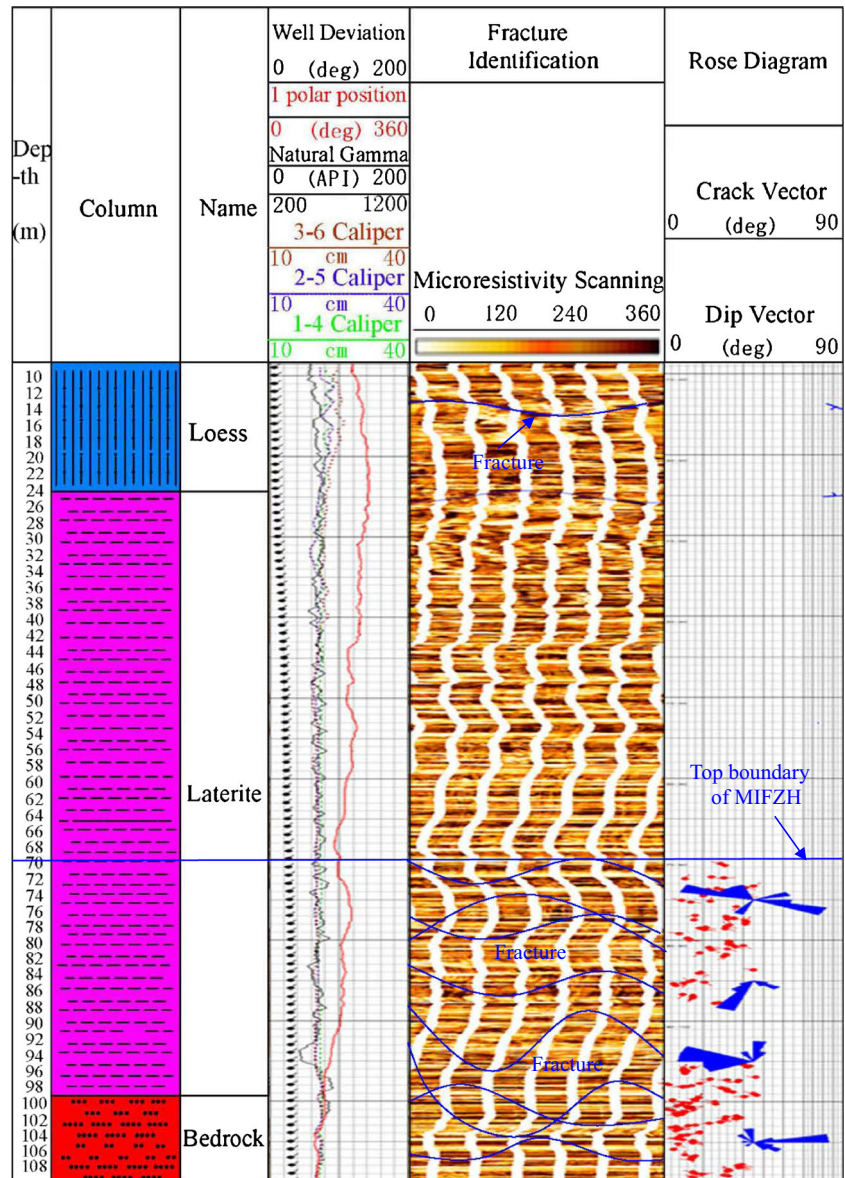
3. The distance from the top boundary of equilibrium arch to surface is $H_g = 22.83 + 76.03 - 30.33 = 68.53$ m $>$ 60.66 m $= 2 \times 30.33$, which satisfied the existing condition of equilibrium arch.
4. MIFZH is $h_{li} = h_{max} + h_b = 30.33 + 120.67 = 151$ m.

On-site measurement

Principle of MRSILT

Micro resistivity scanning imaging logging technology (MRSILT) is an important method of borehole wall imaging (Wu 2000; Jia et al. 2000), which uses the small button-shaped electrodes on a multi-polar plate to transmit the electric current to the borehole wall strata, and then the electric current

Fig. 7 Scanning image and strata histogram in measured section



changes because of the difference of the rock composition, structure, and fluid contacted by electrodes. The change of current reflects the change of the resistivity of the strata around the borehole wall, which can describe the structure, lithology, and fracture characteristics of the strata according to the borehole wall imaging, as shown in Fig. 6. Therefore, MRSILT is applied to test MIFZH in laterite.

Results of field test

Figure 7 showed the scanning image and strata histogram in measured section. There was a downward fracture in the 14 m of drilling depth in loess, which may be caused by mining activities (Huang et al. 2010). With the increase of drilling depth, there were no fractures in the strata until the drilling depth reached 70 m. Drilling depth continued to increase, while fractures density increased. Therefore, drilling depth of 70 m was considered as top boundary of MIFZH. In addition, the buried depth of coal seam was 219.53 m, and therefore, MIFZH was 149.53 m.

Developed in Neogene laterite, MIFZH is 151 and 149.53 m in theoretical analysis and field test, respectively, where the two results are basically consistent and verified the feasibility of theoretical analysis and MRSILT.

Conclusions

1. In theoretical analysis of MIFZH developed in bedrock, based on theory of plate and shell, the overlying each stratum of coalface stress decreasing zone was simplified as four clamped rectangular plates, and the value of the ultimate deflection of the thin plate and the height of the free space in the lower part of the stratum was compared to judge that the MIFZH of 12-2up0101 coalface in Jinjitan colliery was 126.56 m. Compared with measured result of MIFZH 126.4 m, it was reasonable for theoretical analysis.
2. Developed in Neogene Laterite, MIFZH was 151 m based on Pu's theory and rock mass limit equilibrium theory.
3. MRSILT, overcoming the shortage of fluid leakage technology, was introduced to detect MIFZH developed in Neogene Laterite, where the measured result was 149.53 m. Compared with the theoretical results, the two results were basically consistent and verified the feasibility of theoretical analysis.

This research provides a reference for water conservation mining under similar conditions.

Acknowledgements The authors would like to express their gratitude to everyone who provided assistance for the present study. This research

was financially supported by the Fundamental Research Funds for the Central Universities of China (Grant No. 2017XKZD07).

References

- Chai HC, Li WP (2014) Analysis of developing mechanism of water transmitting fractured zone mining approaching to weathered and oxidized zone. *Chin J Rock Mech Eng* 33(7):1319–1328
- Chen RH, Bai HB, Feng MM (2006) Determination of the height of water flowing fractured zone in overburden strata above fully-mechanized top-coal caving face. *J Min Saf Eng* 23(2):220–223
- Fan GW, Zhang DS, Ma LQ (2011) Overburden movement and fracture distribution induced by longwall mining of the shallow coal seam in the Shendong coalfield. *J Chin Univ Min Technol* 40(2):196–201
- Gao YF (1996) “Four-zone” model of rock mass movement and back analysis displacement. *J China Coal Soc* 21(1):51–56
- Gao YF, Huang WP, Liu GL, Zhang SF, Zhu QM, Deng ZY (2012) The relationship between permeable fractured zone and rock stratum tensile deformation. *J Min Saf Eng* 29(3):301–306
- Hu XJ, Li WP, Cao DT, Liu MC (2012) Index of multiple factors and expected height of fully mechanized water flowing fractured zone. *J China Coal Soc* 37(4):613–620
- Huang KZ (1987) Theory of plate and shell. Tsinghua University press, Beijing, pp 112–114
- Huang QX, Wei BN, Zhang WZ (2010) Study of downward crack closing of clay aquiclude in shallowly buried coal seam. *J Min Saf Eng* 27(1):39–43
- Jia WY, Tian SY, Sun YT (2000) Imaging logging technology and its application. Petroleum Industry Press, Beijing
- Juan LB (1996) Mathcad. Editorial Club Universitario, Alicante, pp 66–67
- Li WP, Duan ZH, Hua JM, Ye GJ, Zhao XJ, Yang HK (2000a) Evaluation of present geological environment and prediction of its variation caused by mining in Yushenfu mine area of north Shaanxi. *J Eng Geol* 8(3):324–333
- Li WP, Ye GJ, Zhang L (2000b) Study on the engineering geological conditions of protected water resources during coal mining action in Yushenfu mine area in the north Shaanxi Province. *J China Coal Soc* 25(5):449–454
- Li T, Li WP, Chang JY, Du PP, Gao Y (2011) Permeability features of water-resistant clay layer in northern Shaanxi province while shallowly buried coal mining. *J Min Saf Eng* 28(1):127–131 137
- Liu XS, Tan YL, Ning JG, Tian C, Wang J (2015) The height of water-conducting fractured zones in longwall mining of shallow coal seams. *Geotech Geol Eng* 33(3):693–700. <https://doi.org/10.1007/s10706-015-9851-2>
- Liu SL, Li WP, Wang QQ, He JH, Xue S (2017) Water intrusion risk zoning and water conservation mining technology in the shennan mining area, Shaanxi, China. *Arab J Sci Eng*. <https://doi.org/10.1007/s13369-017-2858-7>
- Majdia A, Hassani FP, Yousef NM (2012) Prediction of the height of distressed zone above the mined panel roof in longwall coal mining. *Int J Coal Geol* 98:62–72. <https://doi.org/10.1016/j.coal.2012.04.005>
- Miao XX, Cui XM, Wang JA, Xu J (2011) The height of fractured water-conducting zone in undermined rock strata. *Eng Geol* 120(1–4):32–39. <https://doi.org/10.1016/j.enggeo.2011.03.009>
- Ning JG, Liu XS, Tan YL, Wang J, Zhang M, Zhang L (2015) Water-preserved mining evaluation in shallow seam with sandy mudstone roof. *J Min Saf Eng* 32(5):814–820
- Palchik V (2003) Formation of fractured zones in overburden due to longwall mining. *Environ Geol* 44(1):28–38. <https://doi.org/10.1007/s00254-002-0732-7>

- Qian MG, Shi PW, Xu JL (2010) Ground pressure and strata control. China University of Mining and Technology Press, Xuzhou, pp 86–87
- Qiao W, Li WP, Li T, Chang JY, Wang QQ (2017) Effects of coal mining on shallow water resources in semiarid regions: a case study in the Shennan Mining Area, Shaanxi, China. *Mine Water Environ* 36(1): 104–113
- Shi LQ, Xin HQ, Zhai PH, Li SC, Liu TB, Yan Y (2012) Calculating the height of water flowing fracture zone in deep mining. *J China Univ Min Technol* 41(1):37–41
- Sun YJ, ZM X, Dong QH (2009) Monitoring and simulation research on development of water flowing fractures for coal mining under xiaolangdi reservoir. *Chin J Rock Mech Eng* 28(2):238–245
- Tan XS, Xian XF (1994) Composite rock mass mechanics theory and its application. Coal Industry Press, Beijing, pp 77–78
- Wang LG, Wang ZS, Huang JH, Zhou DL (2012) Prediction on the height of water-flowing fractured zone for shallow seam covered with bed-rock and thick windblown sands. *J Min Saf Eng* 29(5):607–612
- Wang G, Wu MM, Wang R, Xu H, Song X (2016) Height of the mining-induced fractured zone above a coal face. *Eng Geol.* <https://doi.org/10.1016/j.enggeo.2016.11.024>
- Wei JC, Wu FZ, Xie DL, Yin HY, Guo JB (2016a) Development characteristic of water flowing fractured zone under semi-cemented medium-low strength country rock. *J China Coal Soc* 41(4):974–983
- Wei JC, Wu FZ, Yin HY, Guo JB, Xie DL (2016b) Formation and height of the interconnected fractures zone after extraction of thick coal seams with overburden in western China. *Mine Water Environ.* <https://doi.org/10.1007/s10230-016-0396-2>
- Wu WS (2000) Geological application of formation microscanner logging. *China Offshore Oil Gas* 14(6):438–441
- Wu Q, Guo XM, Shen JJ, Xu S, Liu S, Zeng Y (2016a) Risk assessment of water inrush from aquifers underlying the Gushuyuan coal mine, China. *Mine Water Environ* 36(1):96–103. <https://doi.org/10.1007/s10230-016-0410-8>
- Wu Q, Xu K, Zhang W (2016b) Further research on “three maps-two predictions” method for prediction on coal seam roof water bursting risk. *J China Coal Soc* 41(6):1341–1347
- Xu ZL (1982) Elastic mechanics. People’s Education Press, Beijing
- Xu JL, Wang XZ, Liu WT, Wang Z (2009) Effects of primary key stratum location on height of water flowing fracture zone. *Chin J Rock Mech Eng* 28(2):380–385
- Yan ZD (2013) Innovation and practice of new mechanized mining equipment and technology. Coal Industry Press, Beijing
- Yao XR, Zhu YH (2012) Coal mine drilling technology and safety. Metallurgical Industry Press, Beijing, pp 125–127
- Zhang MS, Dang XY (2014) Water resources and environmental problems in arid and semi arid regions—analysis of Yulin energy and chemical base in northern Shaanxi. Science Press, Beijing
- Zhang DS, Fan GW, Ma LQ, Wang A, Liu YD (2009) Harmony of large-scale underground mining and surface ecological environment protection in desert district—a case study in Shendong mining area, northwest of China. *Procedia Earth Planet* 1:1114–1120
- Zhang W, Zhang DS, LX W, Wang HZ (2014) On-site radon detection of mining-induced fractures from overlying strata to the surface: a case study of the baoshan coal mine in China. *Energies* 7(12):8483–8507. <https://doi.org/10.3390/en7128483>
- Zhang Y, Ye JH, Ji HG, Wang JN (2016) Identifying the development of mining-induced fractures zone using dynamic stress tracing method. *Rock Soil Mech* 37(11):3291–3323
- Zhao BC, Liu ZR, Tong C, Wang C (2015) Relation between height of water flowing fractured zone and mining parameters. *J Min Saf Eng* 32(4):634–638